

# Planning with Learned Dynamics: Guaranteed Safety and Reachability via Lipschitz Constants

Craig Knuth<sup>\*1</sup>, Glen Chou<sup>\*1</sup>, Necmiye Ozay<sup>1</sup> and Dmitry Berenson<sup>1</sup>

**Abstract**—We present an approach for feedback motion planning of systems with unknown dynamics which provides guarantees on safety, reachability, and stability about the goal. Given a learned control-affine approximation of the true dynamics, we estimate the Lipschitz constant of the difference between the true and learned dynamics to determine a trusted domain for our learned model. Provided the system has at least as many controls as states, we further derive the conditions under which a one-step feedback law exists. This allows for a small bound on the tracking error when the trajectory is executed on the real system. Our method imposes a check for the existence of the feedback law as constraints in a sampling-based planner, which returns a feedback policy ensuring that under the true dynamics, the goal is reachable, the path is safe in execution, and the closed-loop system is invariant in a small set about the goal. We demonstrate our approach by planning using learned models of a 6D quadrotor and a 7DOF Kuka arm. We show that a baseline which plans using the same learned dynamics *without* considering the error bound or the existence of the feedback law can fail to stabilize around the plan and become unsafe.

## I. INTRODUCTION

Planning and control with guarantees on safety and reachability for systems with unknown dynamics has long been sought-after in the robotics and control community. Model-based optimal control can achieve this if the dynamics are precisely modeled, but modeling assumptions inevitably break down when applied to real physical systems due to unmodeled effects from friction, slip, flexing, etc. To account for this gap, data-driven machine learning methods and robust control seek to sidestep the need to precisely model the dynamics *a priori*. While robust control can provide strong guarantees when the unmodeled component of the dynamics is small and satisfies strong structural assumptions [1], such methods requires an accurate prior which may not be readily available. In contrast, machine learning methods are flexible but are often brittle and lack formal guarantees, precluding their use in safety-critical applications. For instance, small perturbations from training data cause drastically poor and costly predictions in stock prices and power consumption [2]. Since even small perturbations from the training distribution can yield untrustworthy results, applying AI systems to predict dynamics can lead to unsafe, unpredictable behavior.

To address this gap, we propose a method for planning with learned dynamics which yields guarantees on safety, reachability, and invariance about the goal in execution on the true system. Our core insight is that we can determine

where a learned model can be trusted for planning using the Lipschitz constant of the error (the difference between the true and learned dynamics), which also informs how well the training data covers the task-relevant domain. Under the assumption of deterministic true dynamics, we can plan trajectories in this trusted domain with strong safety guarantees for an important class of learned dynamical systems.

Specifically, with a Lipschitz constant, we can bound the difference in dynamics between a novel point (that our model was not trained on) and a training point. Since the bound grows with the distance to training points, we can naturally define a domain where the model can be trusted as the set of points within a certain distance to training points. Conversely, to obtain a small bound over a desired domain, it is necessary to have good training data coverage. At a high level, to obtain a small bound on the error in a domain, we want to have good coverage over the domain and regularity of the learned model via the Lipschitz constant of the error.

If the learned dynamics have at least as many controls as states and are control-affine (note we do *not* assume the true dynamics are also control-affine), then we also determine conditions for the existence of a feedback controller that tightly tracks the planned trajectory in execution under the true dynamics. The tight tracking error bound yields favorable properties for our planner and controller: 1) it guarantees safety if no obstacle is within the tracking error of the trajectory, 2) it guarantees we can reach the goal within a small tolerance, and 3) if we can assert a feedback law keeping the system at the goal exists, then the closed-loop system is guaranteed to remain in a small region around the goal. In this paper, we assume the learned dynamics are control-affine, deterministic, and have at least as many controls as states, and that the true dynamics are deterministic. If these assumptions are satisfied, then our method guarantees safety, reachability, and invariance about the goal as long as the learned model is sufficiently accurate. Our contributions are:

- 1) A method to bound error between two general dynamics functions in a domain by using a Lipschitz constant
- 2) A condition for uncertain control-affine systems that guarantees the existence of a feasible feedback law
- 3) A planning approach that guarantees safety and closed-loop stability-like properties about the goal for learned dynamics that have at least as many controls as states
- 4) Evaluation on a 7DOF Kuka arm and a 6D quadrotor

<sup>\*</sup>C. Knuth and G. Chou contributed equally to this work

<sup>1</sup>All authors affiliated with the University of Michigan, Ann Arbor, MI 48109, US, {cknuth, gchou, necmiye, dmitryb}@umich.edu

## II. RELATED WORK

Two existing methods combine the ideas of using both coverage of data and regularization with Lipschitz constants to guarantee properties of the resulting learned function; however neither are applied to problems in learning dynamics. In [3], the authors seek to learn a control barrier function (CBF) from data. The authors ensure the CBF is valid through regularity of the Lipschitz constant and checking that it satisfies necessary conditions at a finite number of training points. Moreover, [4] approximates a nonlinear state estimator with a linear state estimator. The authors estimate the maximum slope (closely related to the Lipschitz constant) of the error and show that, with bounded training error, the approximation generalizes. In contrast, our method is a novel application to planning with learned dynamics, which we further extend by incorporating an error bound in planning to provide safety, reachability, and stability-like guarantees.

More broadly, our work is related to methods for planning and control of unknown dynamics with performance guarantees. A traditional approach is robust control, which assumes a good prior on the true dynamics and that unmodeled components are tightly bounded in some set [1]. Robust control has been applied in model predictive control [5] and Hamilton-Jacobi (HJ) reachability analysis [6]. While these methods have strong guarantees, the assumption that the unmodeled dynamics can be tightly bounded requires a accurate prior whereas our method does not, by actively keeping both planned and executed trajectories in a domain where the model can be trusted without *a priori* knowledge.

More recent work focuses on using Gaussian Processes (GPs) to estimate the mean and covariance of the dynamics. With the system dynamics modeled as a GP, various probabilistic bounds on safety and reachability are possible. For example, [7] probabilistically bounds the reachable set of a fixed horizon trajectory. Similarly [8] presents a method to explore the environment while ensuring (with some probability) safety by applying HJ reachability analysis. In a variety of contexts, GPs are used to derive confidence bounds that can be used to provide probabilistic guarantees on safety [9] [10]. These methods are capable of modeling dynamics with stochasticity in contrast to our method which requires deterministic dynamics. However, the methods that rely on GPs are incapable of long-horizon planning due to the unbounded growth of the covariance ellipse unless a known feedback controller exists. Our method does not require any prior controller, and we can plan trajectories of arbitrary length without unbounded growth of the reachable set.

Some recent work explores the challenge of long-horizon planning with learned models, but none offer guarantees of safety or reachability. [11] attempts to plan trajectories in learned latent spaces applied to humanoid robots. [12] learns the capability of an existing controller by estimating the confidence that it can navigate between two nearby robot configurations, and then uses that confidence when connecting adjacent configurations in a sampling-based planner. Similarly, [13] learns when to trust a reduced-order dynamics

model for planning. Again, our method provides guarantees on safety and reachability where none of these methods do.

Our safety guarantees rely on guaranteeing the existence of a stabilizing feedback controller in execution, which is similar to LQR-trees [14], funnel libraries [15], and planning with LQGs [16]. Unlike these approaches, our method requires no *a priori* model and does not make structural assumptions on the true dynamics (i.e. that they are polynomial), and is still able to guarantee the existence of a feedback law.

## III. PRELIMINARIES

Let  $f : \mathcal{X} \times \mathcal{U} \rightarrow \mathcal{X}$  be the true unknown discrete-time dynamics where  $\mathcal{X}$  is the state space and  $\mathcal{U}$  is the control space, which we assume are deterministic. Let  $\mathcal{S} = \{(x_i, u_i, f(x_i, u_i))\}_{i=1}^N$  be the training data for  $g$ . Let  $\Psi = \{(x_j, u_j, f(x_j, u_j))\}_{j=1}^M$  be another set of samples collected near  $\mathcal{S}$  that will be used to estimate the Lipschitz constant. A single state-control pair is written as the tuple  $(x, u)$ . With some abuse of notation, we write  $(x, u) \in \mathcal{S}$  if  $(x, u) = (x_i, u_i)$  from some  $1 \leq i \leq N$  (similarly for  $\Psi$ ). Let  $g : \mathcal{X} \times \mathcal{U} \rightarrow \mathcal{X}$  be an approximation of the true dynamics that is control-affine and therefore can be written as follows

$$g(x, u) = g_0(x) + g_1(x)u. \quad (1)$$

In this paper, we represent the approximate dynamics with a learned neural network model, though in general this approximation is agnostic to the structure of the model and how the model is derived.

A Lipschitz constant bounds how much outputs change with respect to a change in the inputs. For some function  $h$ , a Lipschitz constant over a domain  $\mathcal{Z}$  is any number  $L$  such that for all  $z_1, z_2 \in \mathcal{Z}$

$$\|h(z_1) - h(z_2)\| \leq L\|z_1 - z_2\| \quad (2)$$

Norms  $\|\cdot\|$  are always the 2-norm or induced 2-norm. We define  $L_{f-g}$ ,  $L_{g_0}$ , and  $L_{g_1}$  as the smallest Lipschitz constants of the error  $f - g$ ,  $g_0$ , and  $g_1$ . The input to  $f - g$  is a state-control pair  $(x, u)$  and its output is a state  $x'$ . For  $g_0$ , both the input and output are a state. For  $g_1$ , its input is a state and its output is a  $\dim(\mathcal{X}) \times \dim(\mathcal{U})$  matrix where  $\dim(\cdot)$  is the dimension of the space. A ball  $\mathcal{B}_r(x)$  of radius  $r$  about a point  $x$  is defined as the set  $\{y \mid \|y - x\| < r\}$ , also referred to as a  $r$ -ball about  $x$ . We suppose the state space  $\mathcal{X}$  is partitioned into safe  $\mathcal{X}_{\text{safe}}$  and unsafe  $\mathcal{X}_{\text{unsafe}}$  sets (e.g., the states in collision with an obstacle).

The method consists of two major components. First, we determine a trusted domain  $D \subseteq \mathcal{X} \times \mathcal{U}$  and estimate the Lipschitz constants. Second, we use  $D$  to find a path to the goal satisfying our safety and reachability requirements. These steps are split into the following two problem statements.

**Problem 1.** *Given a learned model  $g$ , unknown dynamics  $f$ , and datasets  $\Psi$  and  $\mathcal{S}$ , determine the trusted domain  $D$  where the error between  $f$  and  $g$  can be tightly bounded and the Lipschitz constants  $L_{f-g}$ ,  $L_{g_0}$ , and  $L_{g_1}$  in  $D$ .*

**Problem 2.** Given control-affine  $g$ , unknown  $f$ , start  $x_I$ , goal  $x_G$ , goal tolerance  $\lambda$ ,  $D$ ,  $L_{f-g}$ ,  $L_{g_0}$ ,  $L_{g_1}$ , and  $\mathcal{X}_{\text{unsafe}}$ , plan a trajectory  $(x_0, \dots, x_K)$ ,  $(u_0, \dots, u_{K-1})$  such that  $x_0 = x_I$ ,  $x_{k+1} = g(x_k, u_k)$ ,  $K < \infty$ , and  $\|x_K - x_G\| \leq \lambda$ . Additionally, under the true dynamics  $f$ , guarantee that closed loop execution does not enter  $\mathcal{X}_{\text{unsafe}}$ , converges to  $\mathcal{B}_{\epsilon+\lambda}(x_G)$ , and remains in  $\mathcal{B}_{\epsilon+\lambda}(x_G)$  after reaching  $x_K$ .

#### IV. METHOD

Secs. IV-A - IV-B and IV-C - IV-D cover our approaches to Probs. 1 and 2, respectively. In Sec. IV-A, we show how  $L_{f-g}$  can establish a trusted domain and how  $L_{f-g}$  can be estimated in Sec. IV-B. In Sec. IV-C, we design a planner that ensures safety, that the system remains in the trusted domain, and that a feedback law maintaining minimal tracking error exists. We present the full algorithm in Sec. IV-D.

##### A. The trusted domain

For many systems we are only interested in a task-relevant domain, and it is often impossible to collect data everywhere in state space, especially for high-dimensional systems. Hence, it is natural that our learned model is only accurate near training data. With a Lipschitz constant of the error, we can precisely define how accurate the learned dynamics are in a domain constructed from the training data. We note this derivation can also be done for systems without the control-affine assumption on the learned dynamics, and thus it can still be useful for determining where a broader class of learned models can be trusted. However, removing the control-affine structure makes controller synthesis much more difficult, and is the subject of future work.

Consider a single training point  $(x, u)$  and a novel point  $(x', u')$ . We derive a bound on the error between the true and estimated dynamics at  $(x', u')$  using the triangle inequality and Lipschitz constant of the error:

$$\begin{aligned} \|f(x', u') - g(x', u')\| &= \|f(x', u') - g(x', u') - f(x, u) + g(x, u) \\ &\quad + f(x, u) - g(x, u)\| \\ &\leq L_{f-g}\|(x', u') - (x, u)\| + \|f(x, u) - g(x, u)\|. \end{aligned} \quad (3)$$

The above relation describes the error at a novel point, but we can also generalize to any domain  $D$ . Define  $b_T$  to be the dispersion [17] of  $\mathcal{S} \cap D$  in  $D$  and define  $e_T$  to be the maximum training error of the learned model. Explicitly,

$$b_T \doteq \sup_{(x', u') \in D} \min_{(x, u) \in \mathcal{S} \cap D} \|(x', u') - (x, u)\| \quad (4)$$

$$e_T \doteq \max_{(x, u) \in \mathcal{S} \cap D} \|f(x, u) - g(x, u)\| \quad (5)$$

Then, we can uniformly bound the error across the entire set  $D$  to yield a simple and exact relation between  $f$  and  $g$ .

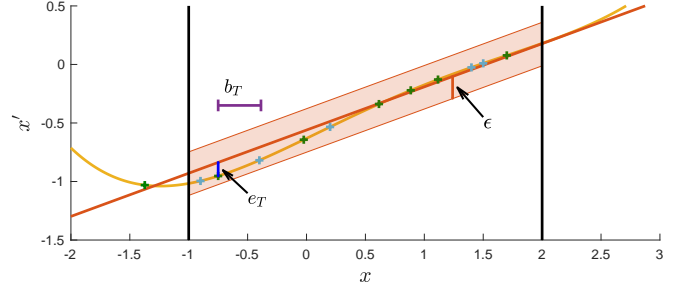


Fig. 1. An example with dynamics  $f(x) = x'$  where  $\dim(\mathcal{X}) = 1$  and  $\dim(\mathcal{U}) = 0$ . The true dynamics are yellow, and the learned linear dynamics are orange.  $\mathcal{S}$  are the green crosses,  $\Psi$  are the light blue crosses, and the domain  $D$  is the interval  $[-1, 2]$  bordered in black. Here,  $b_T = 0.3633$  (purple) and  $e_T = 0.1161$  (blue). The Lipschitz constant of the error here is  $L_{f-g} = 0.1919$  giving  $\epsilon = 0.1859$ . With this bound, we can assert that the difference between the learned and true dynamics is no more than  $\epsilon$  in  $D$ , which is identified by the shaded orange area. Note the Lipschitz of the error,  $L_{f-g}$ , may become larger outside of domain  $D$ .

$$\epsilon \doteq L_{f-g}b_T + e_T \quad (6)$$

$$\forall (x, u) \in D \quad f(x, u) = g(x, u) + \delta, \quad \|\delta\| \leq \epsilon \quad (7)$$

See Fig. 1 for an example of these quantities. In practice, we select  $D$  to be the union of  $r$ -balls about a subset of the training data  $\mathcal{S}_D \subset \mathcal{S}$  as shown below:

$$D = \bigcup_{(x, u) \in \mathcal{S}_D} \mathcal{B}_r(x, u) \quad (8)$$

In the next section we discuss selection of  $\mathcal{S}_D$ , its relation to the estimation of  $L_{f-g}$ , and how  $r$  is selected.

##### B. Estimating the Lipschitz constant

For (7) to hold over the entirety of  $D$ , we require that  $L_{f-g}$  is a Lipschitz constant for the error. Since no assumption is made on the nature of the true dynamics, it is impossible to derive a guaranteed upper bound on  $L_{f-g}$  solely from samples. While the estimation procedure described below (as is done in [4]) almost certainly gives an underestimation of  $L_{f-g}$ , it is sufficient for our experiments. However, more nuanced procedures exist in literature on black box optimization [18]. We approximate  $L_{f-g}$  with the following:

$$\hat{L}_{f-g} = \max_{\substack{(x, u), (x', u') \\ \in (\mathcal{S} \cup \Psi) \cap D}} \frac{\|f(x, u) - g(x, u) - f(x', u') + g(x', u')\|}{\|(x, u) - (x', u')\|} \quad (9)$$

Note that we only estimate the Lipschitz constants using points from  $\Psi$  and  $\mathcal{S}$  that are also in  $D$ . In this way,  $L_{f-g}$  and  $D$  are coupled. We want to choose  $D$  to be large enough for planning while also keeping  $L_{f-g}$  small. To achieve this, we use a filtering procedure to reduce the impact of outliers in  $\mathcal{S}$ . Let  $\mu$  and  $\sigma$  be the mean and standard deviation of the error of the learned model over  $\mathcal{S}$ . Then, let  $\mathcal{S}_D = \{(x, u) \mid \|f(x, u) - g(x, u)\| \leq \mu + a\sigma\}$  where  $a$  is a user-defined parameter. Then, we run Alg. 1 in order to grow

$D$ . This method works by proposing values of  $r$ , estimating  $L_{f-g}$ , and increasing  $r$  until  $r > \epsilon$  or  $L_{f-g} \geq 1$ . Finding  $D$  with  $r > \epsilon$  and  $L_{f-g} < 1$  is useful for planning (described further in Sec. IV-C, see (11)). Note that, in Euclidean spaces,  $r$  is always equal to  $b_T$  since no point in  $D$  is further than a distance  $r$  from  $S_D$  and the furthest any point in  $D$  can lie from a point in  $S_D$  is  $r$ . This algorithm will terminate, as the set  $(S \cup \Psi) \cap D$  only grows and there is only a finite number of samples.

This filtering allows us to exclude regions of space where our learned model may not be accurate (yielding smaller  $e_T$ ) and, since we do not filter over  $\Psi$ , we do not bias the estimate of  $L_{f-g}$ . It is important to not filter points over  $D$  because this can bias  $\hat{L}_{f-g}$  to be a more significant underestimate of the true  $L_{f-g}$ . We note that this algorithm provides a minimum value for  $r$ , but larger values can be selected to improve planning performance. A larger  $r$  makes sampling easier by increasing the size of the trusted domain.

---

**Algorithm 1:** Selecting  $r$  and  $D$

---

**Input:**  $\mu, \sigma, a, S_D, \Psi, \alpha > 0$

---

```

1  $r \leftarrow \mu + a\sigma$ 
2  $\text{done} \leftarrow \text{false}$ 
3 while not  $\text{done}$  do
4   construct  $D$  using equation (8)
5   estimate  $L_{f-g}$  using equation (9)
6   calculate  $\epsilon$  using equation (6)
7   if  $r > \epsilon$  or  $L_{f-g} \geq 1$  then  $\text{done} \leftarrow \text{true}$ 
8   else  $r \leftarrow \epsilon + \alpha$  //  $\alpha$  is a small
      constant

```

---

While the assumption that the true dynamics are deterministic is never explicitly addressed in our method, the estimated Lipschitz constant may be unbounded in the stochastic case, such as when two samples have the same inputs but different outputs due to noise, causing a division by 0 in (9).

$L_{g_0}$  and  $L_{g_1}$  may be estimated by (9). Alternatively, recent work in estimating the Lipschitz constant of neural networks can give tight upper bounds on the Lipschitz constant, e.g. [19], though they generally do not scale to large networks. In our experiments, we estimate the Lipschitz using (9) as our networks were too large to use methods like [19].

### C. Planning

We want to plan a trajectory from start  $x_I$  to goal  $x_G$  using the learned dynamics while remaining in  $\mathcal{X}_{\text{safe}}$  in execution. We constrain the system to stay inside  $D$ , as model accuracy may degrade outside of the trusted domain. We develop a planner similar to a kinodynamic RRT [20], growing a search tree  $\mathcal{T}$  by sampling controls that steer towards novel states until we reach the goal. If a path is found the we can ensure the goal is reachable with safety guarantees.

1) *Staying inside  $D$ :* To remain inside the set  $D$ , we introduce another set  $D_\epsilon := D \ominus \mathcal{B}_\epsilon(0)$ , which is the Minkowski difference between  $D$  and a ball of radius  $\epsilon$ . Every point in  $D_\epsilon$  is at least a distance of  $\epsilon$  from any point

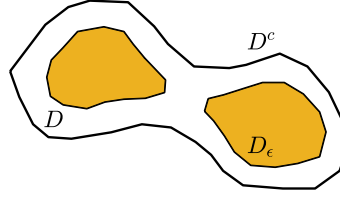


Fig. 2. Visualizing  $D$  (boundary in black),  $D_\epsilon$  (yellow), and  $D^c$  (complement of  $D$ ). Each point in  $D_\epsilon$  is at least  $\epsilon$  distance away from  $D^c$ . If the system is controlled to a point in  $D_\epsilon$  from anywhere in  $D$  under the learned dynamics, then it remains in  $D$  under the true dynamics.

in the complement of  $D$ . Since the learned dynamics differs from the true dynamics by at most  $\epsilon$  in  $D$ , controlling to a point in  $D_\epsilon$  under the learned dynamics ensures the system remains within  $D$  under the true dynamics (see Fig. 2).

How do we determine if a query point  $(x, u)$  is inside of  $D_\epsilon$ ? Since we define  $D$  to be a union of balls (8), it would suffice to find a subset of training points  $\mathcal{W} \subset S_D$  such that the union of  $b_T$ -balls about the training points completely covers an  $\epsilon$ -ball about  $(x, u)$ . Explicitly,

$$\bigcup_{(x', u') \in \mathcal{W}} \mathcal{B}_{b_T}(x', u') \supset \mathcal{B}_\epsilon(x, u) \quad (10)$$

In general, checking (10) is difficult, but if  $L_{f-g} < 1$  and

$$b_T > \frac{e_T}{1 - L_{f-g}}, \quad (11)$$

then only one training point within a distance  $b_T - \epsilon$  is needed to ensure a query point is in  $D_\epsilon$  (see Fig. 3). Note by Alg. 1 line 7, either (11) is guaranteed or  $L_{f-g} \geq 1$ .

**Lemma 1.** *If  $L_{f-g} < 1$  and  $b_T$  is selected according to equation (11), then a point  $(x, u)$  is in  $D_\epsilon$  if there exists  $(x', u') \in S$  such that  $\|(x, u) - (x', u')\| \leq b_T - \epsilon$ .*

*Proof.* To prove, note we can rearrange terms in equation (11) to get  $b_T > L_{f-g}b_T + e_T = \epsilon$ . If there exists  $(x', u') \in S_D$  such that  $\|(x, u) - (x', u')\| \leq b_T - \epsilon$ , then  $\mathcal{B}_\epsilon(x, u) \subset \mathcal{B}_{b_T}(x', u') \subset D$  since no point in  $\mathcal{B}_\epsilon(x, u)$  is further than  $b_T$  distance from  $(x', u')$ . Since  $\mathcal{B}_\epsilon(x, u) \subset D$ ,  $(x, u)$  is at least  $\epsilon$  distance from any point in  $D^c$  and therefore  $(x, u) \in D_\epsilon$ .  $\square$

In order to ensure  $L_{f-g} < 1$ , since it is derived from the training data and learned model, we must train a learned model that is sufficiently accurate (i.e. low error on  $S \cup \Psi$ ). In our experiments, it was enough to minimize mean squared error over the training set to learn models with this property.

To ensure that the resulting trajectory remains in  $D_\epsilon$ , we ensure that corresponding pairs of state and control lie in  $D_\epsilon$  at each step. In growing the search tree  $\mathcal{T}$ , we break down this requirement into two separate checks, the first of which optimistically adds states to the search tree and the second that requires pairs of states and controls to lie in  $D_\epsilon$ . To illustrate, suppose we sample a new configuration  $x_{\text{new}}$  and grow the tree from some  $x$  to  $x_{\text{new}}$ . At this point, when sampling a control  $u$  to steer from  $x$  to  $x_{\text{new}}$  we enforce that  $(x, u) \in D_\epsilon$  (see line 11 in Alg. 2). However, how do we know the resulting state,  $x' = g(x, u)$ , will lie in  $D_\epsilon$ ? Since  $x'$  is a state and not a state-control pair, the above question is not well defined. Instead, we perform an optimistic check in

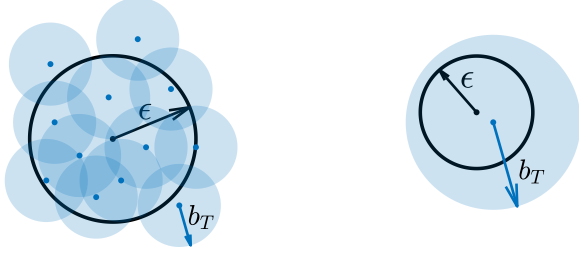


Fig. 3. Illustrating the advantage of  $L_{f-g} < 1$  and  $b_T$  selected according to (11). An  $\epsilon$ -ball about a query point is shown in black;  $b_T$ -balls about training data are shown in blue. **Left:**  $L_{f-g} > 1$ , therefore requiring many training points to cover an  $\epsilon$ -ball about the query point. **Right:**  $L_{f-g} < 1$  and  $b_T$  is selected according to (11). Under these conditions, only one training point within a  $b_T - \epsilon$  distance ensures an  $\epsilon$ -ball about the  $(x, u)$  is entirely in  $D$ , ensuring that the query point is in  $D_\epsilon$ .

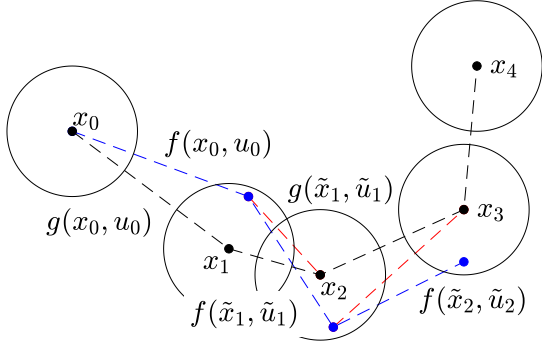


Fig. 4. An illustration of the one-step feedback law. The plan under the learned dynamics is in dashed black, the rollout under the true dynamics is in dashed blue, and the prediction under the learned dynamics using the one step feedback law is in dashed red. At each point, a feedback control  $\tilde{u}_k$  is computed using (13) such that  $x_{k+1} = g(\tilde{x}_k, \tilde{u}_k)$ . Under the true dynamics, the system arrives at some state within an  $\epsilon$ -ball about the next state. The process repeats until the goal is reached.

adding  $x'$  which requires that there exists some  $u''$  such that  $(x', u'') \in D_\epsilon$  (see line 14 in Alg. 2). In turn, when growing the search tree from  $x'$  to some other sampled point  $x'_{\text{new}}$  we ensure that the pair of state and newly sampled control  $u'$  lies in  $D_\epsilon$ , i.e.  $(x', u') \in D_\epsilon$ .

2) *One step feedback law:* To prevent drift in execution, we also seek to ensure the trajectory planned with RRT can be tracked with minimal error. One key requirement to guarantee a feedback law exists is that the system is sufficiently actuated under the learned dynamics. This requires that  $\dim(\mathcal{U}) \geq \dim(\mathcal{X})$ . The check for sufficient actuation is done on a per state basis and can be done as we grow  $\mathcal{T}$ . This feedback law ensures that, under the learned dynamics, we can always return to a planned trajectory in exactly one step when in the trusted domain  $D$ .

Suppose we are executing a trajectory  $(x_0, \dots, x_K)$  with corresponding control  $(u_0, \dots, u_{K-1})$  planned with the learned dynamics, and the system is currently at  $x_{k-1}$ . Under the learned dynamics, the plan is to move to  $x_k = g(x_{k-1}, u_{k-1})$ , but, under the true dynamics, the system will end up at some  $\tilde{x}_k = f(x_{k-1}, u_{k-1})$  which is no more than an  $\epsilon$  distance from  $x_k$ . Our goal is to find an input  $\tilde{u}_k$  such that  $x_{k+1} = g(\tilde{x}_k, \tilde{u}_k)$ . If this one-step feedback law exists

for all  $1 \leq k \leq K-1$ , it ensures the executed trajectory stays within  $\epsilon$  distance of the planned trajectory (see Fig. 4).

With Lipschitz constants  $L_{g_0}$  and  $L_{g_1}$ , we can bound how much the learned dynamics varies in the  $\epsilon$ -ball about  $x_k$ .

$$\forall \tilde{x}_k \in \mathcal{B}_\epsilon(x_k), \quad g(\tilde{x}_k, u) = g_0(x_k) + \Delta_0 + (g_1(x_k) + \Delta_1)u \quad (12)$$

where  $\|\Delta_0\| \leq L_{g_0}\epsilon$  and  $\|\Delta_1\| \leq L_{g_1}\epsilon$ . With (12), the existence of  $\tilde{u}_k$  is informed by a perturbed linear equation:

$$\begin{aligned} x_{k+1} &= g(\tilde{x}_k, \tilde{u}_k), \quad \tilde{x}_k \in \mathcal{B}_\epsilon(x_k) \\ \Rightarrow x_{k+1} &= g_0(x_k) + \Delta_0 + (g_1(x_k) + \Delta_1)\tilde{u}_k \\ \Rightarrow A\tilde{u}_k &= b \end{aligned} \quad (13)$$

with  $A = g_1(x_k) + \Delta_1$  and  $b = x_{k+1} - g_0(x_k) - \Delta_0$

Prior to execution, we seek to answer two questions: when does  $\tilde{u}_k$  exist and does  $\tilde{u}_k$  lie in the control space  $\mathcal{U}$  (for instance in the presence of box constraints)? Results from the literature [21] gives a bound on the difference between the nominal solution  $u_k$  and perturbed solution  $\tilde{u}_k$ .

$$\|u_k - \tilde{u}_k\| \leq \frac{\|g_1(x_k)^+\|(\|\Delta_1\|\|u_k\| + \|\Delta_0\|)}{1 - \|g_1(x_k)^+\|\|\Delta_1\|} \doteq \bar{u}_{\text{pert}} \quad (14)$$

where  $g_1(x_k)^+$  is the pseudo-inverse of  $g_1(x_k)$  (in general  $g_1(x_k)$  is not square). We can use this bound to ensure that  $\tilde{u}_k$  is guaranteed to lie in  $\mathcal{U}$  by enforcing that  $u_k + \bar{u}_{\text{pert}}\mathbf{1}_\infty \subseteq \mathcal{U}$ , where  $\mathbf{1}_\infty$  is the unit infinity-norm ball. Furthermore,  $A$  may become singular if  $1 - \|g_1(x_k)^+\|\|\Delta_1\| \leq 0$ . In this case,  $\tilde{u}_k$  is not guaranteed to exist.

If  $\tilde{u}_k$  exists and satisfies the control constraints for all  $1 \leq k \leq K-1$ , then we ensure that the system will track the path up to an  $\epsilon$  error under the one-step feedback law. In planning, we add the existence of a valid one step feedback law as a check when growing the search tree. Formally:

**Theorem 1.** For trajectory  $(x_0, \dots, x_K)$  and  $(u_0, \dots, u_{K-1})$ , if the solution to the perturbed linear equation (13),  $\tilde{u}_k$ , exists for all  $k \in \{1, \dots, K-1\}$ , then under the true dynamics  $\|\tilde{x}_k - x_k\| \leq \epsilon$  for all  $k$ , given  $L_{f-g}$  is an overestimate of the true Lipschitz constant of  $f - g$ .

*Proof.* Proof by induction. For the induction step, assume  $\|\tilde{x}_k - x_k\| \leq \epsilon$  for some  $k$ . Since  $\tilde{x}_k \in \mathcal{B}_\epsilon(x_k)$ , the perturbed linear equation (13) is valid. If a solution exists, then  $x_{k+1} = g(\tilde{x}_k, \tilde{u}_k)$  and  $\|f(\tilde{x}_k, \tilde{u}_k) - x_{k+1}\| \leq \epsilon$ . This satisfies the induction step. For the base case, we have  $g(x_0, u_0) = x_1$  and  $\|f(x_0, u_0) - x_1\| \leq \epsilon$ . Thus, for all  $k$ ,  $\|\tilde{x}_k - x_k\| \leq \epsilon$ .  $\square$

3) *Ensuring safety and invariance about the goal:* Since it is guaranteed by Thm. 1 that  $\|\tilde{x} - x_k\| \leq \epsilon$ , we check that  $\mathcal{B}_\epsilon(x_k) \subset \mathcal{X}_{\text{safe}}$  for each  $x_k$  on the path to ensure safety.

The exact nature of this check depends on the system and definition of  $\mathcal{X}_{\text{unsafe}}$ . For example, in our experiments on quadrotor, the state includes the quadrotor's position in  $\mathbb{R}^3$

and  $\mathcal{X}_{\text{unsafe}}$  is defined by unions of boxes in  $\mathbb{R}^3$ . By defining a bounding sphere that completely contains the quadrotor, we can verify a path is safe via sphere-box intersection. With the Kuka arm, we randomly sample joint configurations in an  $\epsilon$ -ball about states, transform the joint configurations via forward kinematics, and check collisions in workspace. While this method is not guaranteed to validate the entire ball around a state, in practice no collisions resulted from execution of plans. Another approach computes a free-space bubble [22] around a given state  $x$  and check if it contains  $\mathcal{B}_\epsilon(x)$ , however this is known to be conservative.

To stay near the goal after executing the trajectory, we use the same perturbed linear equation to ensure the existence of a one-step feedback law. Here, rather than checking the next state along the trajectory is reachable from the previous, we check that the final state is reachable from itself, i.e.  $x_K$  is reachable from  $x_K$ . Similar to the arguments above, we can repeatedly execute the feedback law to ensure the system remains in an  $(\epsilon + \lambda)$ -ball about the goal. Formally, we have:

**Theorem 2.** *If the solution, denoted  $u_{\text{st}}$ , to the perturbed linear equation exists for  $A = g_1(x_K) + \Delta_1$  and  $b = x_K - g_0(x_K) - \Delta_0$  for all  $x \in \mathcal{B}_\epsilon(x_K)$ , then the closed loop system will remain in  $\mathcal{B}_{\epsilon+\lambda}(x_G)$ , given  $L_{f-g}$  is an overestimate of the true Lipschitz constant of  $f - g$ .*

*Proof.* By Thm. 1,  $\|\tilde{x}_K - x_K\| \leq \epsilon$ . Thus, if the solution to the perturbed linear equation with  $A = g_1(x_K) + \Delta_1$  and  $b = x_K - g_0(x_K) - \Delta_0$  exists and is valid then  $g(\tilde{x}_K, u_{\text{st}}) = x_K$  and  $\|f(\tilde{x}_K, u_{\text{st}}) - x_K\| \leq \epsilon$ . Since  $\|x_K - x_G\| \leq \lambda$ , the system remains in  $\mathcal{B}_{\epsilon+\lambda}(x_K)$  by the triangle inequality.  $\square$

#### D. Algorithm

We present our full method, **Learned Models in Trusted Domains (LMTD-RRT)**, in Alg. 2. `SampleState` and `SampleControl` sample uniformly in  $\mathcal{X}$  and  $\mathcal{U}$ , though for some systems, we found it useful to sample perturbations from training data and use the control from the nearest state in the training data (see (11)). This does not exclude valid  $(x, u)$  pairs since all points in  $D_\epsilon$  lie within  $b_T - \epsilon$  from a training point and each point along the trajectory must lie in  $D_\epsilon$ . We define the set  $\mathcal{S}_\mathcal{X} = \{x \mid \exists u \text{ s.t. } (x, u) \in \mathcal{S}_D\}$  to perform the optimistic check described in Sec. IV-C.1. `NN` finds the nearest neighbor and `OneStep` checks that a valid feedback exists as described in Sec. IV-C.2. `Model` evaluates the learned dynamics and `InCollision` checks if an  $\epsilon$ -ball is in  $\mathcal{X}_{\text{safe}}$  as described in Sec. IV-C.3.

Once a plan has been computed, it can be executed in closed-loop with Alg. 3. `ModelG0` and `ModelG1` evaluate  $g_0$  and  $g_1$  of the learned model. `SolveLE` solves the linear equation and `Dynamics` executes the true dynamics  $f$ .

## V. RESULTS

We present results on 1) a 2D system to illustrate the need for remaining near the trusted domain, 2) a 6D quadrotor to show scaling to higher-dimensional systems, and 3) a 7DOF Kuka arm simulated in Mujoco [23] to show scaling

### Algorithm 2: LMTD-RRT

---

**Input:**  $x_I, x_G, \mathcal{S}_\mathcal{X}, \mathcal{S}_D, b_T, \epsilon, \lambda, N_{\text{samples}}, \text{goal\_bias}$

```

1  $\mathcal{T} \leftarrow \{x_I\}$ 
2 while True do
3   while  $\neg \text{sampld}$  do
4      $x_{\text{new}} \leftarrow \text{SampleState}(\text{goal\_bias})$ 
5     if  $\|x_{\text{new}} - \text{NN}(\mathcal{S}_\mathcal{X}, x_{\text{new}})\| \leq b_T - \epsilon$  then
6        $\text{sampld} \leftarrow \text{True}$ 
7    $x_{\text{near}} \leftarrow \text{NN}(\mathcal{T}, x_{\text{new}})$ 
8    $i \leftarrow 0, u_{\text{best}} \leftarrow \emptyset, x_{\text{best}} \leftarrow \emptyset, d \leftarrow \infty$ 
9   while  $i < N_{\text{samples}}$  do
10     $u \leftarrow \text{SampleControl}()$ 
11    if  $\|(x_{\text{near}}, u) - \text{NN}(\mathcal{S}_D, (x_{\text{near}}, u))\| \leq b_T - \epsilon$  then
12       $x_{\text{next}} \leftarrow \text{Model}(x_{\text{near}}, u)$ 
13      if  $\text{OneStep}(x_{\text{near}}, u, x_{\text{next}}) \wedge$ 
14         $\|x_{\text{next}} - \text{NN}(\mathcal{S}_\mathcal{X}, x_{\text{next}})\| \leq b_T - \epsilon \wedge$ 
15         $\|x_{\text{next}} - x_G\| < d \wedge$ 
16         $\neg \text{InCollision}(x_{\text{next}}, \epsilon)$  then
17         $u_{\text{best}} \leftarrow u, x_{\text{best}} \leftarrow x_{\text{next}}$ 
18         $d \leftarrow \|x_{\text{next}} - x_G\|$ 
19     $i \leftarrow i + 1$ 
20  if  $u_{\text{best}}$  then
21     $\mathcal{T} \leftarrow \mathcal{T} \cup \{x_{\text{best}}\}$ 
22    if  $\|x_{\text{best}} - x_G\| \leq \lambda$  then
23      return  $\text{ConstructPath}(\mathcal{T}, x_{\text{best}})$ 
```

---

### Algorithm 3: LMTD-Execute

---

**Input:**  $\{x_k\}_{k=0}^K, \{u_k\}_{k=0}^{K-1}$

```

1  $\tilde{x}_0 \leftarrow x_0, k \leftarrow 0$ 
2 for  $k = 1 \dots n - 1$  do
3    $b \leftarrow x_{k+1} - \text{ModelG0}(\tilde{x}_k)$ 
4    $A \leftarrow \text{ModelG1}(\tilde{x}_k)$ 
5    $\tilde{u}_k \leftarrow \text{SolveLE}(A, b)$ 
6    $\tilde{x}_{k+1} \leftarrow \text{Dynamics}(\tilde{x}_k, \tilde{u}_k)$ 
```

---

to complex dynamics that are not available in closed form. We plan with LMTD-RRT, and rollout those plans in open-loop (no computation of  $\tilde{u}_k$ ) and closed-loop (Alg. 3). We compare our method to a naïve kinodynamic RRT skipping the checks on lines 5, 11, 13-14 of Alg. 2. We execute the baseline plans in open loop and with a closed loop controller minimizing distance to the next state under the learned dynamics. Please see the video for experiment visualizations.

#### A. 2D Sinusoidal Model

To aid in visualization, we demonstrate LMTD-RRT on a 2D system with dynamics  $f(x, u) = f_0(x) + f_1(x)u$ :

$$f_0(x) = \begin{bmatrix} x \\ y \end{bmatrix} + \Delta T \begin{bmatrix} 3 \sin(0.3(x + 4.5)) \sin(0.3(y + 4.5)) \\ 3 \sin(0.3(y + 4.5)) \sin(0.3(x + 4.5)) \end{bmatrix}$$

$$f_1(x) = \Delta T \begin{bmatrix} 1 + 0.05 \cos(y) & 0 \\ 0 & 1 + 0.05 \sin(x) \end{bmatrix}$$



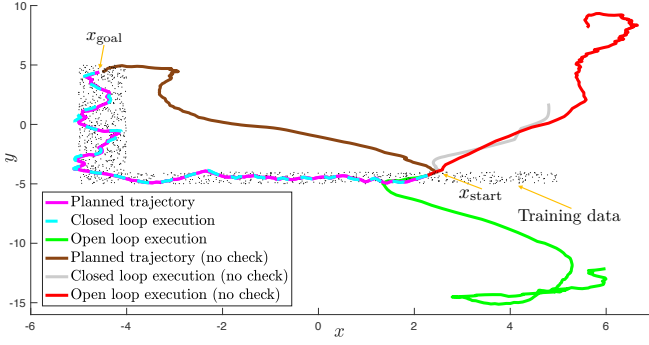


Fig. 5. 2D sinusoidal dynamics. LMTD-RRT generates the magenta plan, staying in  $D$  and ensuring that a valid feedback law exists at each step. The closed loop trajectory (cyan) tracks the plan within  $\epsilon$ . If the feedback law is not applied, the system drifts to the edge of the trusted domain, exits, and then rapidly diverges from the plan (green). In contrast, the naïve RRT plans to the goal without considering  $D$  (brown), and neither the closed loop (grey) or open loop (red) trajectories reach the goal.

where  $\Delta T = 0.2$ . We are given 9000 training points  $(x_i, u_i, f(x_i, u_i))$ , where  $x_i$  is drawn uniformly from an ‘L’-shaped subset of  $\mathcal{X}$  (see Fig. 5) and  $u_i$  is drawn uniformly from  $\mathcal{U} = [-1, 1]^2$ .  $g_0(x)$  and  $g_1(x)$  are modeled with separate neural networks with one hidden layer of size 128 and 512, respectively. 1000 more points are used to estimate  $L_{f-g}$  with Alg. 1, for  $a = 3$ . We obtain  $\epsilon = 0.279$  over  $D$ .

See Fig. 5 for examples of the nominal, open-loop, and closed-loop trajectories planned with LMTD-RRT and a naïve kinodynamic RRT. The plan computed with LMTD-RRT remains in regions where we can trust the learned model (i.e. within  $D_\epsilon$ ) and the closed-loop execution of the trajectory converges to  $\mathcal{B}_{\epsilon+\lambda}(x_G)$ . In contrast, both the open-loop and closed-loop execution of the naïve RRT plan diverge. We provide statistics in Table I of maximum  $\ell_2$  tracking error  $\max_{i \in \{1, \dots, T\}} \|\tilde{x}_i - x_i\|$  and final  $\ell_2$  distance to the goal  $\|\tilde{x}_T - x_G\|_2$ , averaged over 70 random start/goal states. To give the baseline an advantage, we fix the start/goal states and plan with naïve RRT using two different dynamics models: 1) the same learned dynamics model used in LMTD-RRT and 2) a learned dynamics model with the same hyperparameters trained on the full dataset ( $10^4$  datapoints), and report the statistics on the minimum of the two errors. The worst case tracking error for the plan computed with LMTD-RRT was 0.163, which is well within the guaranteed tracking error bound of  $\epsilon = 0.279$ , while despite the data advantage, plans computed with naïve RRT suffer from higher tracking error. Average planning times for LMTD-RRT and naïve RRT are 4.5 and 17 seconds, respectively. Overall, this suggests that planning with LMTD-RRT avoids regions where model error may lead to poor tracking, unlike planning with a naïve RRT.

## B. 6D Quadrotor Model

We evaluate our method on 6-dimensional fully-actuated quadrotor dynamics [24] with state  $x = [\chi, y, z, \phi, \theta, \psi]^\top$ ,

	LMTD-RRT	Naïve kino. RRT
Max. trck. err. (CL)	$0.093 \pm 0.028$ (0.163)	$8.759 \pm 4.166$ (15.21)
Goal error (CL)	$0.035 \pm 0.020$ (0.084)	$7.879 \pm 3.828$ (14.78)
Max. trck. err. (OL)	$13.52 \pm 4.597$ (20.47)	$10.39 \pm 1.948$ (15.31)
Goal error (OL)	$13.13 \pm 4.784$ (20.47)	$10.12 \pm 1.749$ (15.20)

TABLE I

SINUSOID ERRORS. MEAN  $\pm$  STANDARD DEVIATION (WORST CASE).

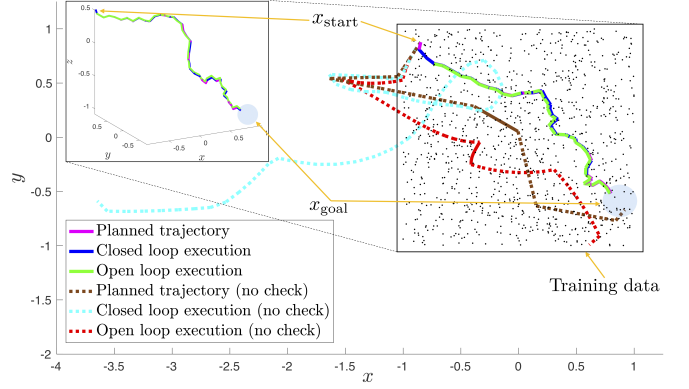


Fig. 6. Quadrotor tracking example. The trajectory planned with LMTD-RRT (magenta) is tracked in closed loop (blue) and reaches the goal. The open loop (green) also converges near the goal, but not as close as the closed loop. The naïve RRT produces a plan (brown) that leaves the trusted domain. Thus, both the open (red) and closed (light blue) loop rapidly diverge.

where  $f(x, u) = f_0(x) + f_1(x)u$ ,  $f_0(x) = x$  and  $f_1(x) =$

$$\Delta T \begin{bmatrix} c_\theta c_\psi & -c_\phi s_\psi + c_\psi s_\phi s_\theta & s_\psi s_\phi + c_\phi c_\psi s_\theta & 0 & 0 & 0 \\ c_\theta s_\psi & c_\phi c_\psi + s_\phi s_\psi s_\theta & -c_\psi s_\phi + c_\phi s_\psi s_\theta & 0 & 0 & 0 \\ -s_\theta & c_\theta s_\phi & c_\phi c_\theta & 0 & 0 & 0 \\ 0 & 0 & 0 & 1 & s_\phi t_\theta & c_\phi t_\theta \\ 0 & 0 & 0 & 0 & c_\phi & -s_\phi \\ 0 & 0 & 0 & 0 & s_\phi c_\theta & c_\phi / c_\theta \end{bmatrix},$$

where  $\Delta T = 0.1$  and  $s(\cdot)$ ,  $c(\cdot)$ , and  $t(\cdot)$  are short for  $\sin(\cdot)$ ,  $\cos(\cdot)$ , and  $\tan(\cdot)$  respectively. We are given  $9 \times 10^6$  training data tuples  $(x_i, u_i, f(x_i, u_i))$ , where  $x_i$ ,  $u_i$  are generated with Halton sampling over  $[-1, 1]^3 \times [-\frac{\pi}{20}, \frac{\pi}{20}]^3$  and  $[-1, 1]^6$ , respectively (i.e the data is collected near hover). As  $f_0(x)$  is a simple integrator term, we assume it is known and set  $g_0(x) = x$ , while  $g_1(x)$  is learned with a neural network with one hidden layer of size 4000. An additional  $1 \times 10^6$  points are used to estimate  $L_{f-g}$ , and we obtain  $\epsilon = 0.097$ .

See Fig. 6 for examples of the planned, open-loop, and closed-loop trajectories planned with LMTD-RRT and a naïve RRT. The trajectory planned with LMTD-RRT remains close to the training data, and the closed-loop system tracks the planned path with  $\epsilon$ -accuracy converging to  $\mathcal{B}_{\epsilon+\lambda}(x_G)$ . We note that using the feedback controller to track trajectories planned with naïve RRT tends to worsen the tracking error, implying our learned model is highly inaccurate outside of the domain. We provide statistics in Table II for maximum tracking error and distance to goal, averaged over 100 random start/goal states. The worst case closed-loop tracking error for trajectories planned with LMTD-RRT is 0.011, again much smaller than  $\epsilon$ . As with the 2D example, we give the baseline an advantage in computing tracking error statistics by reporting the minimum of the two errors

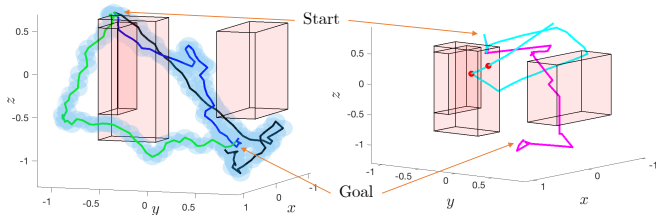


Fig. 7. **L**: Quadrotor obstacle (red) avoidance. Example plans (green, blue, black), tracking error bound  $\epsilon$  overlaid (light blue). Closed-loop trajectories remain in the tubes, converging to the goal without colliding. **R**: Naïve RRT plan (pink) fails to be tracked (cyan) and collides (red dots).

	LMTD-RRT	Naïve kino. RRT
Max. trck. err. (CL)	$0.006 \pm 0.002$ (0.011)	$10.59 \pm 16.75$ (153.26)
Goal error (CL)	$0.003 \pm 0.002$ (0.010)	$8.247 \pm 8.434$ (46.150)
Max. trck. err. (OL)	$0.037 \pm 0.016$ (0.103)	$4.289 \pm 2.340$ (12.986)
Goal error (OL)	$0.034 \pm 0.017$ (0.102)	$3.265 \pm 2.028$ (11.670)

TABLE II

QUADROTOR ERRORS (NO OBSTACLES). MEAN  $\pm$  STDEV (WORST CASE).

when planning with 1) the same model used in LMTD-RRT and 2) a model trained on the full dataset ( $10^7$  points). Despite the data advantage, the plans computed using naïve RRT have much higher tracking error. Average planning times for our unoptimized code are 100 sec. for LMTD-RRT and 15 min. for naïve RRT, suggesting that sampling focused near the training data can improve planning efficiency.

We also evaluate LMTD-RRT on an obstacle avoidance problem (Fig. 7). We perform collision checking as described in Sec. IV-C.3. As the tracking error tubes (of radius  $\epsilon = 0.097$ ) centered around the nominal trajectories never intersect with any obstacles, we can guarantee that the system never collides in execution. Empirically, in running Alg. 2 over 500 random seeds to obtain different nominal paths, the closed-loop trajectory never collides. In contrast, the naïve RRT plan fails to be tracked and collides (Fig. 7, right).

### C. 7DOF Kuka Arm in Mujoco

We evaluate our method on a 7DOF Kuka iiwa arm simulated in Mujoco [23] using a Kuka model from [25]. We train two models using different datasets, one for evaluating tracking error without the presence of obstacles (Table III), and the other for obstacle avoidance. For both models,  $g_0(x)$  is again set to be  $x$  while  $g_1(x)$  is learned with a neural network with one hidden layer of size 4000. For the results in Table III, we are provided 2475 training data tuples, which are collected by recording continuous state-control trajectories and evaluating  $f(x, u)$  on the trajectories and on random state-control perturbations locally around the trajectories. An additional 275 points are used to estimate  $L_{f-g}$ , and we obtain  $\epsilon = 0.055$ . In Table III, we provide statistics on maximum tracking error and distance to goal under plans with LMTD-RRT and the naïve RRT baseline (with a model trained on the full dataset of 2750 points), averaged over 25 runs of each algorithm. Notably, closed-loop tracking of plans generated with LMTD-RRT have

	LMTD-RRT	Naïve kino. RRT
Max. trck. err. (CL)	$0.008 \pm 0.009$ (0.036)	$0.090 \pm 0.250$ (1.265)
Goal error (CL)	$0.003 \pm 0.003$ (0.012)	$0.082 \pm 0.251$ (1.265)
Max. trck. err. (OL)	$0.030 \pm 0.035$ (0.132)	$0.076 \pm 0.084$ (0.282)
Goal error (OL)	$0.030 \pm 0.035$ (0.131)	$0.071 \pm 0.075$ (0.225)

TABLE III

7DOF ARM ERRORS (NO OBSTACLES). MEAN  $\pm$  STDEV (WORST CASE).

lowest error, with the worst case error much smaller than  $\epsilon = 0.055$ . Planning takes on average 0.782 and 0.167 sec. for LMTD-RRT and naïve RRT, respectively.

For the obstacle avoidance example (Fig. 8), we are provided 15266 datapoints, which again take the form of continuous trajectories plus perturbations. An additional 1696 points are used to estimate  $L_{f-g}$ , and we obtain  $\epsilon = 0.085$ . In planning, as described in Sec. IV-C.3, we perform collision checking by randomly sampling configurations in an  $\epsilon$ -ball about each point along the trajectory. Though this collision checker is not guaranteed to detect collision, in running LMTD-RRT over 20 random seeds, we did not observe collisions in execution for any of the 20 plans, and the arm safely reaches the goal without collision. Over these trajectories, the worst case tracking error is 0.081, which remains within  $\epsilon = 0.085$ . One such plan computed by LMTD-RRT and the corresponding open-loop and closed-loop tracking trajectories, is shown in the top row of Fig. 8. The three trajectories nearly overlap exactly due to small tracking error. In contrast, the naïve RRT plan cannot be accurately tracked, even with closed-loop control, due to planning outside of the trusted domain, causing the executed trajectories to diverge and collide with the table.

## VI. DISCUSSION AND CONCLUSION

We present a method to bound the difference between learned and true dynamics in a given domain and also derive conditions that guarantee a one-step feedback law exists. We combine these two properties to design a planner that can guarantee safety, goal reachability, and that the closed-loop system remains in a small region about the goal.

While the method presented has strong guarantees, it also has limitations which are interesting targets for future work. First, the true dynamics are assumed to be deterministic. Stochastic dynamics may be possible by modifying the approach to approximate the Lipschitz constant of the mean dynamics while also appropriately modeling the noise. Second, the actuation requirement limits the systems that this method can be applied to. For systems with  $\dim(\mathcal{U}) < \dim(\mathcal{X})$ , it may be possible to construct a similar feedback law that guarantees the learned dynamics will lie within a tolerance of planned states which, in turn, could still give strong guarantees on safety and reachability.

## REFERENCES

- [1] K. Zhou and J. C. Doyle, *Essentials of robust control*, 1998.
- [2] G. R. Mode and K. A. Hoque, “Adversarial examples in deep learning for multivariate time series regression,” 2020.



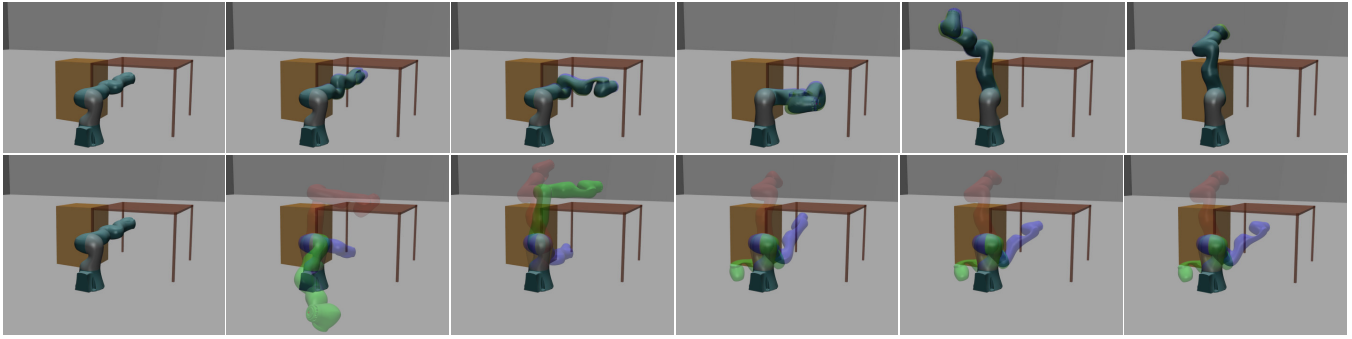


Fig. 8. Planning to move a 7DOF arm from below to above a table. Trajectory-tracking time-lapse (time increases from left to right). Red (nominal), green (closed loop), blue (open loop). **Top:** LMTD-RRT (red, green, blue overlap due to tight tracking). **Bottom:** Naïve RRT (poor tracking causes collision).

- [3] A. Robey, H. Hu, L. Lindemann, H. Zhang, D. V. Dimarogonas, S. Tu, and N. Matni, "Learning control barrier functions from expert demonstrations," 2020.
- [4] S. Dean, N. Matni, B. Recht, and V. Ye, "Robust guarantees for perception-based control," in *LADC*, 2020, pp. 350–360.
- [5] A. Aswani, H. Gonzalez, S. S. Sastry, and C. Tomlin, "Provably safe and robust learning-based model predictive control," *Automatica*, vol. 49, no. 5, pp. 1216–1226, 2013.
- [6] I. M. Mitchell, A. M. Bayen, and C. J. Tomlin, "A time-dependent hamilton-jacobi formulation of reachable sets for continuous dynamic games," *TAC*, vol. 50, no. 7, pp. 947–957, 2005.
- [7] T. Koller, F. Berkenkamp, M. Turchetta, and A. Krause, "Learning-based model predictive control for safe exploration," in *CDC*, 2018, pp. 6059–6066.
- [8] A. K. Akametalu, J. F. Fisac, J. H. Gillula, S. Kaynama, M. N. Zeilinger, and C. J. Tomlin, "Reachability-based safe learning with gaussian processes," in *CDC*, 2014, pp. 1424–1431.
- [9] F. Berkenkamp, R. Moriconi, A. P. Schoellig, and A. Krause, "Safe learning of regions of attraction for uncertain, nonlinear systems with gaussian processes," in *CDC*, 2016, pp. 4661–4666.
- [10] F. Berkenkamp, M. Turchetta, A. Schoellig, and A. Krause, "Safe model-based reinforcement learning with stability guarantees," in *NeurIPS*, 2017, pp. 908–918.
- [11] B. Ichter and M. Pavone, "Robot motion planning in learned latent spaces," *IEEE RA-L*, vol. 4, no. 3, pp. 2407–2414, 2019.
- [12] J. Guzzi, R. O. Chavez-Garcia, M. Nava, L. M. Gambardella, and A. Giusti, "Path planning with local motion estimations," *IEEE Robotics and Automation Letters*, vol. 5, no. 2, pp. 2586–2593, 2020.
- [13] D. McConachie, T. Power, P. Mitrano, and D. Berenson, "Learning when to trust a dynamics model for planning in reduced state spaces," *IEEE RA-L*, vol. 5, no. 2, pp. 3540–3547, 2020.
- [14] R. Tedrake, "Lqr-trees: Feedback motion planning on sparse randomized trees," *Robotics: Science and Systems V*, 2009.
- [15] A. Majumdar and R. Tedrake, "Funnel libraries for real-time robust feedback motion planning," *IJRR*, vol. 36, no. 8, pp. 947–982, 2017.
- [16] J. Van Den Berg, P. Abbeel, and K. Goldberg, "Lqg-mp: Optimized path planning for robots with motion uncertainty and imperfect state information," *IJRR*, vol. 30, no. 7, pp. 895–913, 2011.
- [17] S. LaValle, *Planning algorithms*. Cambridge university press, 2006.
- [18] D. E. Kvasov and Y. D. Sergeyev, "Lipschitz global optimization methods in control problems," *Automation and Remote Control*, vol. 74, no. 9, pp. 1435–1448, 2013.
- [19] M. Fazlyab, A. Robey, H. Hassani, M. Morari, and G. Pappas, "Efficient and accurate estimation of lipschitz constants for deep neural networks," in *NeurIPS*, 2019, pp. 11 427–11 438.
- [20] S. M. LaValle and J. J. Kuffner Jr, "Randomized kinodynamic planning," *IJRR*, vol. 20, no. 5, pp. 378–400, 2001.
- [21] P. Lötstedt, "Perturbation bounds for the linear least squares problem subject to linear inequality constraints," *BIT Numerical Mathematics*, vol. 23, no. 4, pp. 500–519, 1983.
- [22] S. Quinlan, *Real-time modification of collision-free paths*. Stanford University Stanford, 1994, no. 1537.
- [23] E. Todorov, T. Erez, and Y. Tassa, "Mujoco: A physics engine for model-based control," in *IROS*, 2012, pp. 5026–5033.
- [24] F. Sabatino, "Quadrotor control: modeling, nonlinear control design, and simulation," 2015.
- [25] "Harvardagileroboticslab/gym-kuka-mujoco." [Online]. Available: <https://github.com/HarvardAgileRoboticsLab/gym-kuka-mujoco>